Macromolecules

Article

pubs.acs.org/Macromolecules

Re-entrance of Poly(*N*,*N*-diethylacrylamide) in D_2O/*d*-Ethanol Mixture at 27 °C

Di Jia,[†,‡] Taisen Zuo,[†,‡] Sarah Rogers,[§] He Cheng,[*,†,‡] Boualem Hammouda,[*,∥] and Charles C. Han[*,⊥]

[†]China Spallation Neutron Source (CSNS), Institute of High Energy Physics (IHEP), Chinese Academy of Sciences (CAS), Dongguan 523803, China

[‡]Dongguan Institute of Neutron Science (DINS), Dongguan 523808, China

[§]ISIS-STFC, Rutherford Appleton Laboratory, Chilton, Oxon OX11 0QX, U.K.

[∥]Center for Neutron Research, National Institute of Standards and Technology, Gaithersburg, Maryland 20899-6102, United States

[⊥]Institute for Advanced Study, Shenzhen University, Shenzhen 518060, China

Supporting Information

ABSTRACT: The re-entrance of poly(*N*,*N*-diethylacrylamide) (PDEA) in D_2O/*d*-ethanol mixtures (i.e., the coil-to-spherical aggregates-to-coil transition) has been observed at 27 °C by small-angle neutron scattering (SANS). PDEA has a lower critical solution temperature (LCST) phase diagram in the D_2O-rich region and is soluble in the D_2O-poor region for all of the observed temperature ranges. Its spinodal temperature decreases first from 33.5 °C in pure D_2O to 26.7 °C in 80% D_2O/20% *d*-ethanol and then increases to 283.1 °C in 50% D_2O/50% *d*-ethanol. With the further decrease of D_2O content, PDEA dissolves well, and its phase boundary can no longer be observed by SANS. Therefore, at 27 °C, PDEA dissolves as random coils when the D_2O content is higher than 90% and then collapses and aggregates to form the globule phase in 20% D_2O/80% *d*-ethanol; finally, it reswells and behaves as random coils again with excluded volume in the D_2O-poor region. The ternary random phase approximation model (RPA) is used to analyze the SANS profiles, and three Flory–Huggins interaction parameters ($\chi_{PDEA-d\text{-ethanol}}$, χ_{PDEA-D_2O}, and $\chi_{d\text{-ethanol}-D_2O}$) are obtained. When a small amount of *d*-ethanol is added to the system, it has a strong interaction with D_2O, so it directly gets distributed into the water structure and makes a negative contribution to the dissolution of PDEA ($\chi_{d\text{-ethanol}-D_2O}$ is much smaller than $\chi_{PDEA-d\text{-ethanol}}$ and χ_{PDEA-D_2O}). With the addition of more *d*-ethanol, its interaction with water becomes weaker, but still stronger than those between PDEA–D_2O and PDEA–*d*-ethanol. Neither *d*-ethanol nor D_2O wants to help the dissolution of PDEA in the first place, until the structure of mixed solvents tends to be pure *d*-ethanol in the D_2O-poor region.

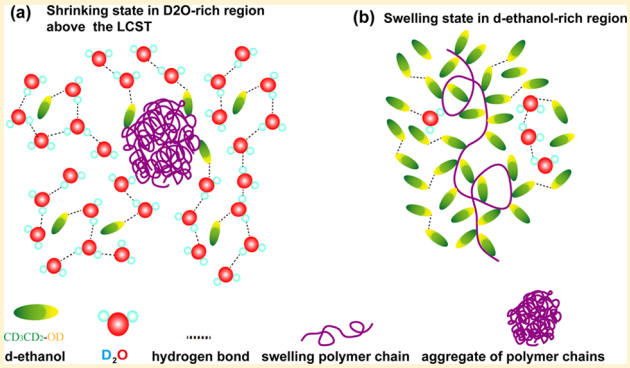

1. INTRODUCTION

Co-nonsolvency is a rare phenomenon for which the solubility of a polymer decreases or even vanishes in the mixture of good solvents.[1] It is an effect which many polymers encounter, and it is one of the interesting questions to what extent there is a universal concept, which describes this phenomenon in general, or whether the situation is different in each case. Even in the case of the latter, a thorough classification would be very helpful for the design of new stimuli-responsive polymers. Poly(*N*-isopropylacrylamide) (PNIPAM) is a typical example. It is soluble in (cold) water and various organic solvents, such as methanol, ethanol, tetrahydrofuran (THF), dioxane, and so on, but cannot dissolve in their binary mixtures.[2] A re-entrant swelling–shrinking–swelling transition with the fraction of organic solvent was observed in PNIPAM gels.[3] On the contrary, PDEA obeys cosolvency in most of the mixtures at room temperature. The absent amide proton in the PDEA side group was thought to be the key for this difference,[4] although PDEA and PNIPAM gels show the same re-entrance behavior in water/dimethyl sulfoxide (DMSO) mixtures.[3]

The origin of co-nonsolvency has been argued for decades. There are four different explanations, i.e., the perturbation of solvent–solvent interaction parameters with the presence of polymer network,[5] "competitive adsorption",[6−10] the formation of a stoichiometric compound between the solvent molecules,[11−14] and strong intersolvent interactions (such as concentration fluctuation in mixed solvent).[15] The first view holds that the re-entrant phase transition occurs because the presence of polymer network enhanced the attractive interaction for alcohol and water.[5] Schild et al.[16] thereby

Received: April 15, 2016
Revised: June 30, 2016
Published: July 13, 2016

DOI: 10.1021/acs.macromol.6b00785
Macromolecules 2016, 49, 5152−5159

questioned this argument when comparing the similar re-entrance phenomenon in both PNIPAM aqueous solutions and gels. The second focuses on the competition between polymer−water (p−w) hydrogen bonds and polymer−organic solvent (like methanol, p−o) hydrogen bonds.[6] Once the first water molecule successfully forms a hydrogen bond with an amide group on a chain, it will cause some displacement of the isopropyl group and create more access space for the next molecule, so the second water molecule can more easily form a bond than the first one, the competition becomes stronger with cooperativity, and small differences in the composition of the mixed solvent will be greatly amplified. Kremer et al. applied the adaptive resolution scheme (AdResS) method with a Metropolis particle exchange criterion to the reentrant behavior of PNIPAM in aqueous methanol and found that the origin of the re-entrance is due to the preferential solute−solvent interactions. In the concentration range where polymer collapses into globule, the average number of hydrogen bonds between PNIPAM and solvent molecules decreases about 20%.[17−19] Note that this assumption assumes the solvent−solvent interaction is so weak, compared to the solvent−polymer interaction, that they can be neglected. The third stresses that the solvent−solvent interaction is so strong that a stoichiometric compound between them is formed, which should be considered as a new "bad solvent"; thereby the polymer cannot be dissolved. For example, Zhang et al.[11,20] used both static and dynamic light scattering to prove that PNIPAM chain exhibits a coil−globule−coil transition in water/methanol mixtures as methanol increases, and they speculated such a transition is induced by the formation of water/methanol complexation. However, direct evidence of such complexation still lacks. The fourth explanation points out that the strong solvent−solvent interactions, such as concentration fluctuation, prevent the solvent−polymer interaction, resulting in the co-nonsolvency. Hao et al.[15] combined SANS, light scattering, and viscometry to prove that the composition fluctuation in THF−water mixture gets a maximum at 20 mol % THF content, and such a composition fluctuation leads to the collapse of PNIPAM-*co*-PEG microgel in the THF−water mixture solvent. Freed et al. refined the classic Flory−Huggins (FH) theory to consider the mutual association of the solvent molecules, and they found that a large negative solvent−solvent interaction parameter is a necessary condition for the occurrence of co-nonsolvency in ternary polymer solutions.[21,22]

Although lots of experiments, e.g., laser light scattering,[20] fluorescence correlation spectroscopy,[23] ellipsometry,[24] etc., and various simulations, such as molecular dynamics[19] and quantum mechanical calculation,[25] have been conducted, the puzzle remains.

There are two key points need to be clarified in order to understand the origin of co-nonsolvency from a thermodynamic point of view. First, the structure of mixed solvents at the molecular level of a few angstroms scale should be connected with the conformation of polymer with dimensions of several nanometers. Note that the polymer−mixed-solvent solution is a single system, not only the entropy variation of the bound water around the polymer but also the structure change of the whole solvent should be considered.[12] Second, three different pairs of interaction parameters (polymer−solvent 1, polymer−solvent 2, and solvent 1−solvent 2) should be measured to evaluate the contribution from different interactions. Recently, SANS was used to study the co-nonsolvency of PNIPAM in D_2O/*d*-ethanol mixture.[26] It was found that PNIPAM has an LCST phase diagram in the D_2O-rich region and an upper critical solution temperature (UCST) phase diagram in the D_2O-poor region. Three-component RPA was applied to fit the SANS profiles; $\chi_{PNIPAM-d\text{-ethanol}}$, $\chi_{PNIPAM-D_2O}$, and $\chi_{d\text{-ethanol}-D_2O}$ were obtained in the D_2O-poor region to reveal the mechanism of co-nonsolvency. Unfortunately, RPA can only be used to fit the data in the one-phase region, but not too far from the phase boundary. The profiles in the D_2O-rich region cannot be analyzed because the corresponding spinodal line of the LCST branch is generally much lower than 0 °C, which makes SANS measurement difficult. And the nonsolvency of PNIPAM in the middle of the phase diagram, e.g., 20%−60% ethanol aqueous solutions, makes it impossible to derive the three interaction parameters in moderate temperature ranges, which leads to a discontinuous, nonlinear of the Flory−Huggins interaction parameters.

All these difficulties motivated us to study the temperature and concentration dependence of the conformation variations of PDEA in the D_2O/*d*-ethanol mixture because PDEA has no amine proton and is soluble in the mixture in moderate temperature ranges. On one hand, the phase behavior of PDEA should be relatively similar to that of PNIPAM if mixed solvent structure really plays an important role in co-nonsolvency, since the only difference in the molecular structures of PDEA and PNIPAM is the amide proton, which is also important for its solubility. On the other hand, three-component RPA can be easily used in PDEA D_2O/*d*-ethanol mixture, which is usually thought to be a typical cosolvency system at room temperature.[27] Our SANS experiments prove that PDEA has also an LCST type phase diagram in the D_2O-rich region, with a critical point at 26.7 °C in 80% D_2O/20% *d*-ethanol; no concentration fluctuations can be observed in the D_2O-poor region by SANS, which implies that the system is extremely stable to have no SANS measurable thermal fluctuation. Three-component RPA fittings verify these findings. The interaction parameter between *d*-ethanol and D_2O is smaller than 0, and much smaller than those of PDEA−*d*-ethanol and PDEA−D_2O, which hints that the interaction between the binary-solvent mixture is predominant in the re-entrance behavior.

2. EXPERIMENTAL SECTION

2.1. Material. PDEA was synthesized by reversible addition−fragmentation chain transfer polymerization (RAFT) according to the literature.[28,29] The molar ratio of the reactants for DEA monomer:CDB (cumyl dithiobenzoate) (chain transfer agent):AIBN (initiator) was 600:1:0.2. 9.9500 g of DEA, 0.0355 g of CDB, and 0.0043 g of AIBN were dissolved in 10 mL of DMF; the mixture was added in a polymerization tube. The tube was first frozen and thawed three times to remove oxygen and then put in an oil bath at 60 °C with a stirring speed of 6.7 Hz (6.7 revolutions per second or 400 rpm) for 5.6 h. After reaction, the monomer/polymer mixture was cooled to room temperature, dissolved in acetone (30 mL), and precipitated from hexane (600 mL). Finally, the product was dried in a vacuum oven at room temperature overnight.

2.2. Ultraviolet−Visible (UV−Vis) Spectroscopy. A UV-2450 UV−vis spectrophotometer equipped with a San Ace 60 temperature control unit was used to measure the absorbance and transmittance of the solutions. For the absorption study, the wavelength was scanned from 200 to 800 nm, while the wavelength was set at 632.8 nm for the transmittance experiment. Standard quartz cuvettes with a path length of 10 mm were used.[30]

2.3. Small-Angle Neutron Scattering. SANS was carried out on the Sans2d small-angle diffractometer at the ISIS Pulsed Neutron Source (STFC Rutherford Appleton Laboratory, Didcot, UK).[31,32] A simultaneous scattering vector (Q) range of 0.0036−0.52 $Å^{-1}$ was

DOI: 10.1021/acs.macromol.6b00785
Macromolecules 2016, 49, 5152−5159

achieved utilizing an incident wavelength range of 1.75−14.0 Å and employing an instrument setup of L1 = L2 = 8 m, with the rear 1 m^2 detector offset vertically by 75 mm and sideways by 100 mm. 4% mass fraction PDEA samples were dissolved in a series of D_2O/*d*-ethanol mixtures (100%, 90%, 80%, 70%, 60%, 50%, 40%, 30%, 20%, 10%, and 0% D_2O in D_2O/*d*-ethanol mixture), providing the necessary contrast, and were included in 2 mm path length Hellma quartz cells. The beam diameter was 8 mm. Each raw scattering data set was corrected for the detector efficiency; sample transmission and background scattering were converted to a scattering cross section ($\partial\Sigma(Q)/\partial\Omega$ vs Q) using the instrument-specific software.[33] These data were placed on an absolute scale (cm^{-1}) using the scattering from a standard sample (a solid blend of hydrogenous and perdeuterated polystyrene) in accordance with established procedures.[34]

3. RESULTS AND DISCUSSION

3.1. Calibration of PDEA. PDEA has to be calibrated to prove that it is monodisperse before any discussion about its phase behavior. For a polymer with excluded volume, its form factor is given by[35,36]

$$P(Q) = \frac{1}{\nu U^{1/2\nu}}\gamma\left(\frac{1}{2\nu}, U\right) - \frac{1}{\nu U^{1/\nu}}\gamma\left(\frac{1}{\nu}, U\right) \quad (1)$$

Here, $\gamma(x,U)$ is the lower incomplete gamma function:

$$\gamma\left(\frac{1}{2\nu}, U\right) = \int_0^U \mathrm{d}t\, \exp(-t)t^{x-1} \quad (2)$$

The variable U is given in terms of the scattering variable Q

$$U = \frac{Q^2b^2n^{2\nu}}{6} = \frac{Q^2R_g{}^2(2\nu+1)(2\nu+2)}{6} \quad (3)$$

where b is the statistical segment length, n is the degree of polymerization, and ν is the excluded volume parameter. The radius of gyration has been defined as

$$R_g = \left[\frac{b^2n^{2\nu}}{(2\nu+1)(2\nu+2)}\right]^{1/2} \quad (4)$$

When $\nu = 3/5$, the polymer behaves as a Gaussian coil with excluded volume in its good solvent.[37]

PDEA is dissolved in pure *d*-ethanol and measured at various temperatures (Figure 1). It is a monodisperse random coil with excluded volume in ethanol, whose R_g = 4.5 nm. Note that all of scattering profiles coincide with each other. The PDEA in *d*-ethanol solution is so stable in the temperature scan that no concentration fluctuation can be observed. In fact, the same phenomenon happens when D_2O fractions are lower than 50%, as will be discussed later.

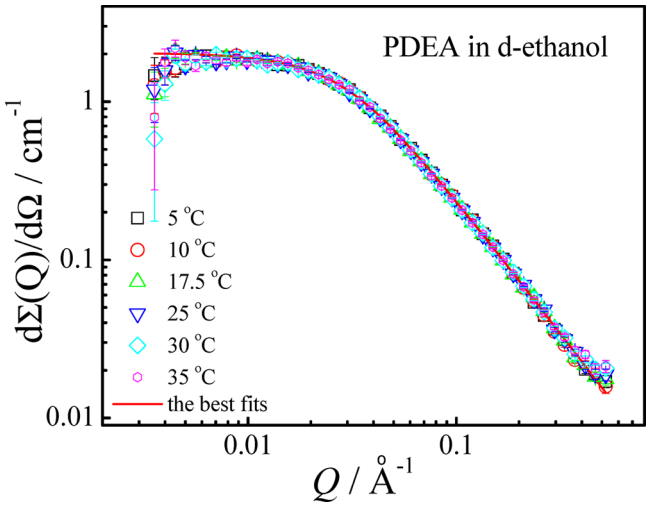

Figure 1. Scattering profiles of 4% mass fraction PDEA in pure *d*-ethanol at various temperatures. The red line is the best fit by eq 1.

3.2. Mapping the Phase Diagram. The phase diagram of PDEA in D_2O/*d*-ethanol mixtures can be deduced from the temperature and concentration dependence of SANS profiles (Figure 2). Evidence of concentration fluctuations can be clearly observed in the D_2O-rich region when its fraction is higher than 50%. Figure 2a shows that the spread is weak in 80% D_2O/20% *d*-ethanol at 5 °C. The amplitude of fluctuation increases with temperature. When it is close to the phase boundary at 25 °C, the fluctuation becomes huge. Concentration (of D_2O) dependence of SANS profiles at room temperature is presented in Figure 2b. Concentration fluctuation increases with the decrease of D_2O fractions when

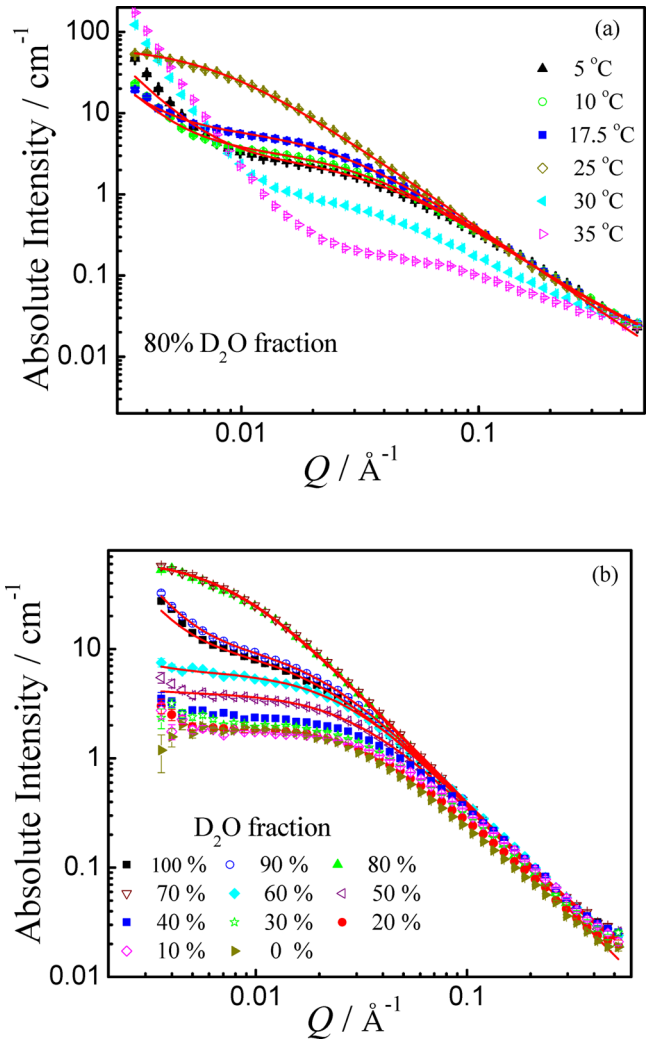

Figure 2. SANS profiles of 4% mass fraction PDEA in *d*-ethanol/D_2O mixtures. (a) Temperature dependence of PDEA in 80% D_2O/20% *d*-ethanol mixture. (b) Concentration dependence of PDEA in D_2O/*d*-ethanol mixtures at 25 °C when D_2O fractions are 100%, 90%, 80%, 70%, 60%, 50%, 40%, 30%, 20%, 10%, and 0%. The red lines are the best fits by eq 5.

DOI: 10.1021/acs.macromol.6b00785
Macromolecules 2016, 49, 5152−5159

Φ_{D_2O} is higher than 20% and then decreases, implying the critical point is at about 20%−30% D_2O fractions.

A simple empirical model is used to fit the SANS profiles when D_2O fractions are between 50% and 100%.[38]

$$\frac{d\Sigma(Q)}{d\Omega} = \frac{A}{Q^n} + \frac{I(0)}{1 + (Q\xi)^m} + \text{background} \quad (5)$$

where $I(0)$ is a characteristic of thermodynamics (susceptibility), ξ is the correlation length, and m is the Porod exponent. A/Q^n only represents the influence of composition fluctuations or self-assembled structure of PDEA because of its hydrophobic head groups at low Q, when the D_2O fraction is higher than 60%.[38] 4% is still lower than the overlapping concentration of PDEA. And it cannot be from any impurities in the system, either, because this small Q scattering totally vanishes when Φ_{D_2O} is lowered. The same phenomenon has been observed in PNIPAM aqueous solutions,[39] where zero average contrast matching was used to explore its origin, and proved that it is from a transient network formation through hydrophobic segment−segment interaction. ξ is the size of concentration fluctuations. The small-angle scattering part increases when the system is close to its phase boundary and has nothing to do with the real size of PDEA coils in solution, which should actually decrease with temperature increase in a LCST system.[40]

Plotting $I(0)^{-1}$ for increasing T^{-1}, where T is the absolute temperature, shows a linear behavior in the one-phase region (Figure 3). A positive slope represents LCST behavior in the

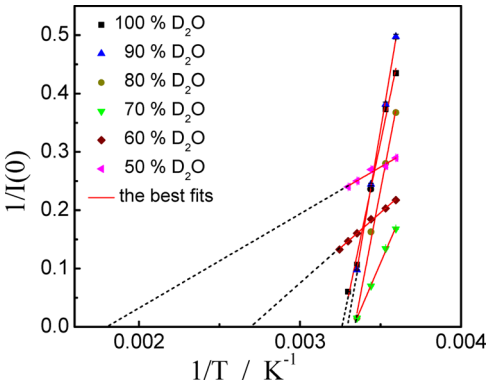

Figure 3. $I(0)^{-1}$ vs T^{-1} of PDEA in D_2O/*d*-ethanol mixtures at various D_2O fractions.

D_2O-rich region. When Φ_{D_2O} is lower than 50%, no temperature dependences of concentration fluctuation can be observed by SANS in the system. It reconfirms that *d*-ethanol is a better solvent for PDEA compared with D_2O. The solution structure will be stable in the temperature range; thereby thermal fluctuations cannot induce any structure variation in the SANS length scale.

The spinodal line can be deduced from the intercept of $I(0)^{-1}$ vs T^{-1} plot, where the extrapolated $I(0)$ diverges. The corresponding UV−vis measurements attest to this as well. Both of them indicate that PDEA is a Gaussian coil with excluded volume when the D_2O fraction is higher than 80%; then it collapses and even aggregates to form globules at Φ_{D_2O} = 80%. A further increase of *d*-ethanol fraction reswells the PDEA globules. It becomes a Gaussian coil with excluded volume again when the D_2O fraction is lower than 70% at 27 °C. The re-entrance behavior of PDEA in D_2O/*d*-ethanol mixtures is similar to that of PNIPAM, which proves that the structure of mixed solvent is one of the most important keys for the conformation variation of polymer in solvent mixture. Besides, the phase diagram of PDEA in water−ethanol mixture was also measured by the UV−vis measurement, and the results show that PDEA has the same phase diagram as that in D_2O/*d*-ethanol mixtures. Therefore, deuteration of the two solvents has little influence on the co-nonsolvency phenomenon.

3.3. Random Phase Approximation. The RPA is a useful tool for the investigation of mixing/demixing thermodynamics of polymer blends[36,41,42] and extended to the case of binary homopolymer and copolymer solutions.[43] Schild et al. were the first to describe co-nonsolvency phenomenon using the Flory−Huggins (FH) type mean field theory.[16] It is applied here to obtain the effective interaction parameters[44] between different species.

To begin with, the boundary (θ) condition in pure D_2O and pure *d*-ethanol has to be calculated. Consider a binary mixture consisting of a mixture of polymers 1 and 2. The absolute scattering intensity at zero scattering angle should be

$$\frac{d\Sigma}{d\Omega} = \Delta\rho^2 S(q \to 0) \quad (6)$$

where $\Delta\rho$ is the difference of scattering length densities, $S(q)$ is the scattering factor, and q is a scattering vector. Then $S(0)$ or the susceptibility can be expressed in a random phase approximation:

$$\frac{1}{S(0)} = \frac{1}{n_1\varphi_1\nu_1} + \frac{1}{n_2\varphi_2\nu_2} - \frac{2\chi_{12}}{\nu_0} \quad (7)$$

Here n_i, φ_i, and ν_i are the degree of polymerization, volume fraction, and specific volume of the different species, χ_{12} is their interaction parameter, and $\nu_0 = (\nu_1\nu_2)^{1/2}$. Thus

$$\frac{\varphi_1}{S(0)} = \frac{1}{n_1\nu_1} + \left[\frac{1}{n_2\varphi_2\nu_2} - \frac{2\chi_{12}}{\nu_0}\right]\varphi_1 \quad (8)$$

The second virial coefficient is defined as

$$A_2 = \left[\frac{1}{2n_2\varphi_2\nu_2} - \frac{\chi_{12}}{\nu_0}\right] \quad (9)$$

The theta condition is defined by $A_2 = 0$

$$\frac{1}{2n_2\varphi_2\nu_2} = \frac{\chi_{12}}{\nu_0} \quad (10)$$

In other words

$$\chi_{12} = \frac{\sqrt{\nu_1}}{2n_2\varphi_2\sqrt{\nu_2}} \quad (11)$$

For solutions, $n_2 = 1$ and usually $\varphi_2 \sim 1$, so

$$\chi_{12} \sim \frac{\sqrt{\nu_1}}{2\sqrt{\nu_2}} \quad (12)$$

Therefore, in PDEA−D_2O solution, the θ condition is obtained for

$$\chi_{PDEA-D_2O} \sim \frac{\sqrt{\nu_1}}{2\sqrt{\nu_2}} = \frac{\sqrt{2.11 \times 10^{-22}}}{2\sqrt{3.00 \times 10^{-23}}} = 1.33$$

while it is

DOI: 10.1021/acs.macromol.6b00785
Macromolecules 2016, 49, 5152−5159

Table 1. Best Fitting Results for the RPA Model According to Eq 15

d-water fraction (%)	E_{12}	F_{12} (K)	E_{13}	F_{13} (K)	E_{23}	F_{23} (K)
90	−1.16 ± 0.00	197.98 ± 0.70	1.86 ± 0.00	−305.63 ± 0.23	0.71 ± 0.00	−112.34 ± 0.48
80	−0.94 ± 0.07	167.19 ± 5.79	1.25 ± 0.09	−213.17 ± 12.30	0.73 ± 0.04	−117.91 ± 8.39
70	−0.60 ± 0.03	78.87 ± 4.08	0.71 ± 0.04	−81.50 ± 2.94	0.53 ± 0.03	−59.18 ± 3.35
60	−0.42 ± 0.00	34.02 ± 0.11	0.44 ± 0.00	−26.65 ± 0.12	0.42 ± 0.00	−23.72 ± 0.13
50	−0.38 ± 0.00	25.58 ± 0.16	0.35 ± 0.00	−15.37 ± 0.22	0.41 ± 0.00	−17.48 ± 0.26

$$\chi_{\text{PDEA}-d\text{-ethanol}} \sim \frac{\sqrt{\nu_1}}{2\sqrt{\nu_2}} = \frac{\sqrt{2.11 \times 10^{-22}}}{2\sqrt{9.68 \times 10^{-23}}} = 0.74$$

in PDEA−d-ethanol solution.

Then the ternary RPA model is described here briefly.[41] The three components thereafter are defined as (1) d-ethanol, (2) D_2O, and (3) PDEA. The corresponding bare structure factors are expressed as $S_{11}^0 = n_1\varphi_1\nu_1$, $S_{22}^0 = n_2\varphi_2\nu_2$, and $S_{33}^0 = n_3\varphi_3\nu_3P(Q)$. $P(Q)$ is the single chain form factor described in eq 1. Note that the cross terms (S_{12}^0, etc.) do not contribute. The following parameters are defined as

$$V_{11} = \frac{1}{S_{33}^0} - \frac{2\chi_{13}}{\nu_{13}}$$

$$V_{22} = \frac{1}{S_{33}^0} - \frac{2\chi_{23}}{\nu_{23}}$$

$$V_{12} = \frac{1}{S_{33}^0} + \frac{2\chi_{12}}{\nu_{12}} - \frac{2\chi_{13}}{\nu_{13}} - \frac{2\chi_{23}}{\nu_{23}} \quad (13)$$

in terms of the Flory−Huggins interaction parameters χ_{12}, χ_{13}, and χ_{23} and the reference volumes $\nu_{12} = (\nu_1\nu_2)^{1/2}$, $\nu_{13} = (\nu_1\nu_3)^{1/2}$, and $\nu_{23} = (\nu_2\nu_3)^{1/2}$. The fully interacting system structure factors can be expressed as

$$S_{11}(Q) = \frac{S_{11}^0(1 + V_{22}S_{22}^0)}{\Delta}$$

$$S_{22}(Q) = \frac{S_{22}^0(1 + V_{11}S_{11}^0)}{\Delta}$$

$$S_{12}(Q) = \frac{S_{11}^0(1 + V_{12}S_{22}^0)}{\Delta} \quad (14)$$

The denominator is given by $\Delta = (1 + V_{11}S_{11}^0)(1 + V_{22}S_{22}^0) - V_{12}^2S_{11}^0S_{22}^0$. The relation $\Delta = 0$ yields the spinodal condition. The SANS macroscopic scattering cross section is given by

$$\frac{d\Sigma(Q)}{d\Omega} = (\rho_1 - \rho_2)^2S_{11}(Q) + (\rho_2 - \rho_3)^2S_{22}(Q) + 2(\rho_1 - \rho_3)(\rho_2 - \rho_3)S_{12}(Q) \quad (15)$$

Here ρ_i is the neutron scattering length density of the ith species.

For the PDEA D_2O/d-ethanol mixture, the following parameters are used:

$$n_1 = n_2 = 1, \quad n_3 = 348, \quad \rho_1 = 6.07 \times 10^{10}\ \text{cm}^{-2} \quad (16a)$$

$$\nu_1 = 9.68 \times 10^{-23}\ \text{cm}^3, \quad \nu_2 = 3.00 \times 10^{-23}\ \text{cm}^3, \quad \nu_3 = 2.11 \times 10^{-22}\ \text{cm}^3 \quad (16b)$$

$$\rho_2 = 6.37 \times 10^{10}\ \text{cm}^{-2}, \quad \rho_3 = 6.20 \times 10^{9}\ \text{cm}^{-2} \quad (16c)$$

The volume fractions of different species can be calculated according to the mass fraction and the density of the mixture. Note that the $1/T$ dependence of the interaction parameters warrants the splitting $\chi_{ij} = E_{ij} + F_{ij}/T$ for all three χ parameters, for a total of six fitting variables in the ternary RPA fitting process. The fitting results are listed in Table 1.

The ternary RPA model was used to fit SANS profiles in Figure 3. Generally, smaller χ means better interactions. In all of the temperature and concentration ranges, $\chi_{d\text{-ethanol}-D_2O}$ are negative and are much smaller than $\chi_{\text{PDEA}-d\text{-ethanol}}$ and $\chi_{\text{PDEA}-D_2O}$ (Figure 5), which clearly indicates that the interaction between water and ethanol dominants in the re-entrance process. At the same temperature, both $\chi_{d\text{-ethanol}-D_2O}$ and $\chi_{\text{PDEA}-D_2O}$ increase, but $\chi_{\text{PDEA}-d\text{-ethanol}}$ decreases with d-ethanol concentration. Thus, PDEA−d-ethanol interaction dominates, while d-ethanol−D_2O and PDEA−D_2O interactions weaken when more ethanol is introduced in the system. Note that all of the three interaction parameters increase or decrease directly without any minimum value which may represent a preferred structure, when the d-ethanol concentration increases. It may prove that there is no perfect stoichiometric structure in the D_2O/d-ethanol mixture. Once d-ethanol is added, it instantaneously interacts with the component it prefers (D_2O in this case). The d-ethanol−D_2O interaction competes with the PDEA−D_2O and PDEA−d-ethanol interactions, leading to the variation of the Gibbs free energy for the whole mixture; the re-entrance behavior thereafter happens to get to a new metastable state. On the other hand, the $\chi_{d\text{-ethanol}-D_2O}$ decreases, but $\chi_{\text{PDEA}-d\text{-ethanol}}$ and $\chi_{\text{PDEA}-D_2O}$ increase with temperature at the same d-ethanol concentration. It demonstrates that the interaction between mixed solvents gets better, but neither of them likes to interact with PDEA at higher temperature, leading to the LCST type of phase diagram in the D_2O-rich region. All of the three sets of slopes for the interaction parameter vs temperature plot (Figure 5) become closer to zero with further increase of d-ethanol concentration, so the conformation of PDEA becomes almost temperature independent in D_2O-poor region, as shown in Figure 1.

One of the interesting observations in Figure 5 is the difference between the measured interaction parameters and its corresponding θ condition (according to eq 12). The PDEA−D_2O interactions are always relatively better than the PDEA−d-ethanol interactions. Therefore, the PDEA−d-ethanol interactions are weaker and thereby cannot compete with PDEA−D_2O interactions at all. The competition in the three-component system happens in the whole mixture once d-ethanol is added, rather than limited to the bound water molecules of PDEA adjacent to its hydrophobic side groups.

It should also be noted that the strong D_2O−d-ethanol interactions are not induced in the presence of PDEA. It has been proposed that the re-entrance behavior can happen if the solvent−solvent interaction parameter is negative.[5,16,45] However, these studies took the view that the actual interaction

DOI: 10.1021/acs.macromol.6b00785
Macromolecules 2016, 49, 5152−5159

parameters between water and alcohol are always positive; thus, there must be a perturbation of solvent−solvent interaction parameter with the presence of a polymer network. Schild et al. thereby questioned this argument when comparing the similar re-entrance phenomenon in both PNIPAM aqueous solutions and gels.[16] Our SANS experiments and the following analysis prove that the solvent−solvent interaction itself is originally strong without the addition of PDEA in bulk water at room temperature, and the negative D_2O−*d*-ethanol interaction parameter leads to the re-entrance behavior directly. As we all know, water and ethanol can form an azeotropic mixture at 78.23 °C, so ethanol cannot be separated from water directly. It partly implies that the water−ethanol interaction is very strong, but whether D_2O and *d*-ethanol could form complexes or not is still an open question. Dixit et al. used neutron diffraction and empirical potential structure refinement (EPSR) to probe the molecular-scale structure of the methanol−water mixture. They concluded that the local structure of water in a concentrated methanol−water solution is close to its counterpart in pure water, and the polar interaction of water with the alcohol hydroxyl group is more important on the thermodynamic properties of the mixed solvent than any water restructuring induced by the hydrophobic alcohol head groups.[46] It is consistent with our observations that D_2O and *d*-ethanol hydrogen bondings are preferentially formed once *d*-ethanol is introduced in the three-component re-entrance system, and there is no stoichiometric compound between D_2O and *d*-ethanol. Therefore, the re-entrance phase diagram in Figure 4 is similar to that of PNIPAM in our previous work.[26]

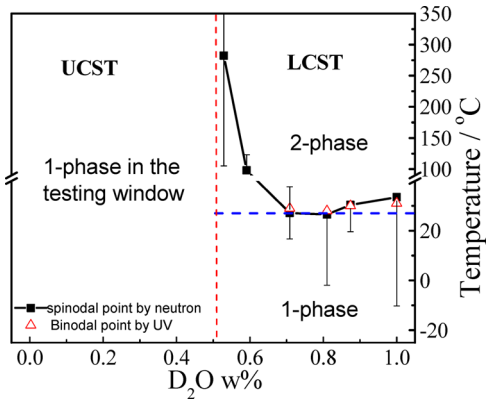

Figure 4. Resultant phase diagram. The black squares are spinodal points, and the red triangular points are cloud points by UV−vis measurements. The blue line indicates where the re-entrance happens at 27 °C.

The strong solvent−solvent interaction is the origin of cononsolvency, and it can induce lots of consequences; e.g., both competitive adsorption and stoichiometric compound may be observed in a co-nonsolvency system. First, competitive interaction can be seen because of strong solvent−solvent interaction. Figure 5 clearly indicates that the PDEA−*d*-ethanol interaction parameters change much more than PDEA−D_2O ones with the increase of *d*-ethanol concentration, which can also be explained that the competition becomes stronger with cooperativity (Although it is just a result of strong *d*-ethanol−D_2O interaction). Second, the stoichiometric compound may not also be necessarily formed. Clusters of water−methanol are found in neutron total scattering experiment,[46] but no obvious

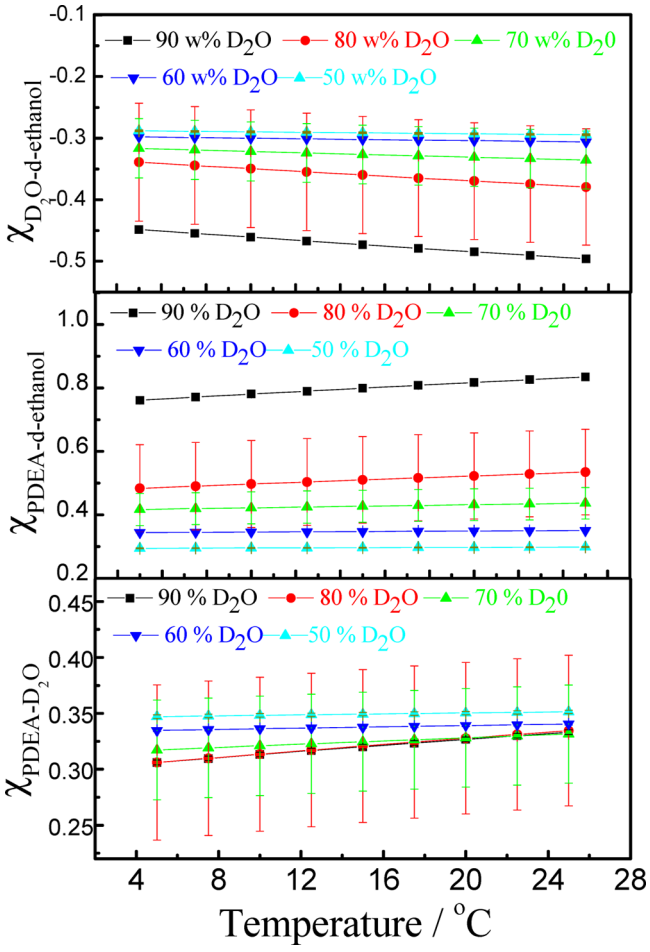

Figure 5. Temperature and *d*-ethanol concentration dependence of three interaction parameters $\chi_{d\text{-ethanol}-D_2O}$, $\chi_{PDEA-d\text{-ethanol}}$, and χ_{PDEA-D_2O}.

water−ethanol clusters are found in the water−ethanol system currently.[47]

The re-entrant behavior can be schematically illustrated in Figure 6. In pure D_2O, PDEA is soluble via hydrogen bonding with bound water. When a small amount of *d*-ethanol is added, the ice-like tetrahedral water structure is not disturbed; *d*-ethanol distributes in the "free volume" inside bulk water and forms strong hydrogen bonding with water so that ethanol

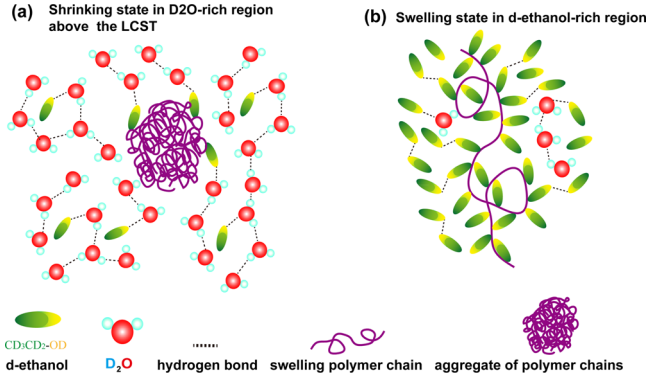

Figure 6. Schematic illustration of shrinking (a) and swelling (b) state in D_2O/*d*-ethanol mixture. The sizes of solvent molecules and polymers in the cartoon are not their real size; they are magnified just for clarity.

DOI: 10.1021/acs.macromol.6b00785
Macromolecules 2016, 49, 5152−5159

cannot interact with PDEA and $\chi_{PDEA-d\text{-ethanol}}$ is large. Therefore, PDEA collapses and aggregates to form globules. The further increase of *d*-ethanol concentration changes the structure of the mixed solvent into zigzag chain structure of neat *d*-ethanol,[47] and there is excess ethanol interacting with PDEA so that PDEA−*d*-ethanol interaction gets better and $\chi_{PDEA-d\text{-ethanol}}$ becomes smaller. Because *d*-ethanol is a better solvent for PDEA than D_2O, PDEA reswell as random coils with excluded volume. This is consistent with the water/ethanol structure observed by Yamaguchi.[47] Their neutron diffraction observation proved that the structure of water/ethanol mixture evolves from bulk water to pure ethanol with the addition of ethanol at the molecular level.

Although both PDEA and PNIPAM show co-nonsolvency in water/DMSO mixture,[3] Richtering et al.[48] studied PDEA and PNIPAM based microgels in water/methanol mixture and found that PNIPAM has a co-nonsolvency effect while PDEA does not. This is partly because the size of the alcohol hydrophobic group plays an important role in co-nonsolvency. A recent study[27] shows that co-nonsolvency of PDEA gel happens in water/alcohol with larger alcohol hydrophobic groups. Cheng et al. used simulations to study the NIPAM/water/methanol system and found the same phenomena.[49] Note that the origin of co-nonsolvency should be universal in the same solvent mixtures if mixed-solvent interaction plays the most important role. So SANS observation should be done in both PNIPAM D_2O/*d*-methanol and PDEA D_2O/*d*-methanol mixtures to evaluate the effects of polymer structure (such as an amine proton) on the origin of co-nonsolvency in the future.

4. CONCLUSIONS

The re-entrance of PDEA in D_2O and *d*-ethanol mixture at 27 °C is studied by SANS. It is found that PDEA has a LCST type of phase diagram in the D_2O-rich region and is totally soluble in the D_2O-poor region. The ternary RPA is used to fit the SANS results, which prove that the preferential interaction between D_2O and *d*-ethanol is the origin of the re-entrance behavior. The mixed solvent changes its structure from pure D_2O to pure *d*-ethanol gradually with the addition of *d*-ethanol; *d*-ethanol molecules prefer to enter the "free volume" of bulk water in the D_2O-rich region, and no stoichiometric compound is formed.

■ ASSOCIATED CONTENT

Supporting Information

The Supporting Information is available free of charge on the ACS Publications website at DOI: 10.1021/acs.macromol.6b00785.

The Porod exponent *m* at different temperatures for 80% D_2O fraction, and the Porod exponent *m* for different D_2O fractions at 25 °C (PDF)

■ AUTHOR INFORMATION

Corresponding Authors

*(H.C.) E-mail chenghe@ihep.ac.cn.
*(B.H.) E-mail hammouda@nist.gov.
*(C.C.H.) E-mail c.c.han@szu.edu.cn.

Notes

The authors declare no competing financial interest.

■ ACKNOWLEDGMENTS

The financial support from the National Basic Research Program of China (973 Program, 2012CB821500), the UK-China Newton project, and National Natural Scientific Foundation of China (No. 21474119) is gratefully acknowledged. The identification of commercial products does not imply endorsement by the National Institute of Standards and Technology nor does it imply that these are the best for the purpose. This work is based upon activities supported in part by the US National Science Foundation under Agreement DMR-1508249.

■ REFERENCES

(1) Cowie, J. M. G.; Mohsin, M. A.; McEwen, I. J. Alcohol-water cosolvent systems for poly(methyl methacrylate). *Polymer* **1987**, *28*, 1569−1572.
(2) Costa, R. O. R.; Freitas, R. F. S. Phase behavior of poly(N-isopropylacrylamide) in binary aqueous solutions. *Polymer* **2002**, *43*, 5879−5885.
(3) Katayama, S.; Hirokawa, Y.; Tanaka, T. Reentrant phase transition in acrylamide-derivative copolymer gels. *Macromolecules* **1984**, *17*, 2641−2643.
(4) Hofmann, C. H.; Plamper, F. A.; Scherzinger, C.; Hietala, S.; Richtering, W. Cononsolvency Revisited: Solvent Entrapment by N-Isopropylacrylamide and N,N-Diethylacrylamide Microgels in Different Water/Methanol Mixtures. *Macromolecules* **2013**, *46*, 523−532.
(5) Amiya, T.; Hirokawa, Y.; Hirose, Y.; Li, Y.; Tanaka, T. Reentrant phase transition of N-isopropylacrylamide gels in mixed solvents. *J. Chem. Phys.* **1987**, *86*, 2375−2379.
(6) Tanaka, F.; Koga, T.; Winnik, F. M. Temperature-Responsive Polymers in Mixed Solvents: Competitive Hydrogen Bonds Cause Cononsolvency. *Phys. Rev. Lett.* **2008**, *101*, 028302.
(7) Walter, J.; Sehrt, J.; Vrabec, J.; Hasse, H. Molecular Dynamics and Experimental Study of Conformation Change of Poly(N-isopropylacrylamide) Hydrogels in Mixtures of Water and Methanol. *J. Phys. Chem. B* **2012**, *116*, 5251−5259.
(8) Kojima, H.; Tanaka, F.; Scherzinger, C.; Richtering, W. Temperature dependent phase behavior of PNIPAM microgels in mixed water/methanol solvents. *J. Polym. Sci., Part B: Polym. Phys.* **2013**, *51*, 1100−1111.
(9) Kyriakos, K.; Philipp, M.; Adelsberger, J.; Jaksch, S.; Berezkin, A. V.; Lugo, D. M.; Richtering, W.; Grillo, I.; Miasnikova, A.; Laschewsky, A.; Müller-Buschbaum, P.; Papadakis, C. M. Cononsolvency of Water/Methanol Mixtures for PNIPAM and PS-b-PNIPAM: Pathway of Aggregate Formation Investigated Using Time-Resolved SANS. *Macromolecules* **2014**, *47*, 6867−6879.
(10) Scherzinger, C.; Balaceanu, A.; Hofmann, C. H.; Schwarz, A.; Leonhard, K.; Pich, A.; Richtering, W. Cononsolvency of mono- and di-alkyl N-substituted poly(acrylamide)s and poly(vinyl caprolactam). *Polymer* **2015**, *62*, 50−59.
(11) Zhang, G.; Wu, C. Reentrant Coil-to-Globule-to-Coil Transition of a Single Linear Homopolymer Chain in a Water /Methanol Mixture. *Phys. Rev. Lett.* **2001**, *86*, 822−825.
(12) Wang, T.; Liu, G.; Zhang, G.; Craig, V. S. J. Insights into Ion Specificity in Water−Methanol Mixtures via the Reentrant Behavior of Polymer. *Langmuir* **2012**, *28*, 1893−1899.
(13) Pang, X.; Wang, K.; Cui, S. Single-chain mechanics of poly(N-isopropyl-acrylamide) in the water/methanol mixed solvent. *Polymer* **2013**, *54*, 3737−3743.
(14) Ebeling, B.; Eggers, S.; Hendrich, M.; Nitschke, A.; Vana, P. Flipping the Pressure- and Temperature-Dependent Cloud-Point Behavior in the Cononsolvency System of Poly(N-isopropylacrylamide) in Water and Ethanol. *Macromolecules* **2014**, *47*, 1462−1469.
(15) Hao, J.; Cheng, H.; Butler, P.; Zhang, L.; Han, C. C. Origin of cononsolvency, based on the structure of tetrahydrofuran-water mixture. *J. Chem. Phys.* **2010**, *132*, 154902.
(16) Schild, H. G.; Muthukumar, M.; Tirrell, D. A. Cononsolvency in mixed aqueous solutions of poly(N-isopropylacrylamide). *Macromolecules* **1991**, *24*, 948−952.
(17) Mukherji, D.; Kremer, K. Coil−Globule−Coil Transition of PNIPAm in Aqueous Methanol: Coupling All-Atom Simulations to

DOI: 10.1021/acs.macromol.6b00785
Macromolecules 2016, 49, 5152−5159

Semi-Grand Canonical Coarse-Grained Reservoir. *Macromolecules* **2013**, *46*, 9158−9163.
(18) Fritsch, S.; Poblete, S.; Junghans, C.; Ciccotti, G.; Delle Site, L.; Kremer, K. Adaptive resolution molecular dynamics simulation through coupling to an internal particle reservoir. *Phys. Rev. Lett.* **2012**, *108*, 170602.
(19) Mukherji, D.; Marques, C. M.; Kremer, K. Polymer collapse in miscible good solvents is a generic phenomenon driven by preferential adsorption. *Nat. Commun.* **2014**, *5*, 4882.
(20) Zhang, G.; Wu, C. The Water/Methanol Complexation Induced Reentrant Coil-to-Globule-to-Coil Transition of Individual Homopolymer Chains in Extremely Dilute Solution. *J. Am. Chem. Soc.* **2001**, *123*, 1376−1380.
(21) Dudowicz, J.; Freed, K. F.; Douglas, J. F. Communication: Cosolvency and cononsolvency explained in terms of a Flory-Huggins type theory. *J. Chem. Phys.* **2015**, *143*, 131101.
(22) Dudowicz, J.; Freed, K. F.; Douglas, J. F. Solvation of polymers as mutual association. II. Basic thermodynamic properties. *J. Chem. Phys.* **2013**, *138*, 164902.
(23) Wang, F.; Shi, Y.; Luo, S.; Chen, Y.; Zhao, J. Conformational Transition of Poly(N-isopropylacrylamide) Single Chains in Its Cononsolvency Process: A Study by Fluorescence Correlation Spectroscopy and Scaling Analysis. *Macromolecules* **2012**, *45*, 9196−9204.
(24) Chen, Q.; Kooij, E. S.; Sui, X.; Padberg, C. J.; Hempenius, M. A.; Schon, P. M.; Vancso, G. J. Collapse from the top: brushes of poly(N-isopropylacrylamide) in co-nonsolvent mixtures. *Soft Matter* **2014**, *10*, 3134−3142.
(25) Scherzinger, C.; Schwarz, A.; Bardow, A.; Leonhard, K.; Richtering, W. Cononsolvency of poly-N-isopropyl acrylamide (PNIPAM): Microgels versus linear chains and macrogels. *Curr. Opin. Colloid Interface Sci.* **2014**, *19*, 84−94.
(26) Hore, M. J. A.; Hammouda, B.; Li, Y.; Cheng, H. Co-Nonsolvency of Poly(n-isopropylacrylamide) in Deuterated Water/Ethanol Mixtures. *Macromolecules* **2013**, *46*, 7894−7901.
(27) Liu, B.; Wang, J.; Ru, G.; Liu, C.; Feng, J. Phase Transition and Preferential Alcohol Adsorption of Poly(N,N-diethylacrylamide) Gel in Water/Alcohol Mixtures. *Macromolecules* **2015**, *48*, 1126−1133.
(28) Idziak, I.; Avoce, D.; Lessard, D.; Gravel, D.; Zhu, X. X. Thermosensitivity of Aqueous Solutions of Poly(N,N-diethylacrylamide). *Macromolecules* **1999**, *32*, 1260−1263.
(29) Hashimoto, C.; Nagamoto, A.; Maruyama, T.; Kariyama, N.; Irisa, Y.; Ikehata, A.; Ozaki, Y. Hydration States of Poly(N-isopropylacrylamide) and Poly(N,N-diethylacrylamide) and Their Monomer Units in Aqueous Solutions with Lower Critical Solution Temperatures Studied by Infrared Spectroscopy. *Macromolecules* **2013**, *46*, 1041−1053.
(30) Wei, G.; Yao, D.; Li, Z.; Huang, Y.; Cheng, H.; Han, C. C. Charge-Transfer Complexation Mechanism of Poly(4-vinylpyridine)/[6,6]-Phenyl-C_{61}-butyric Acid Methyl Ester in DMF Solution. *Macromolecules* **2013**, *46*, 1212−1220.
(31) http://www.isis.stfc.ac.uk.
(32) Heenan, R. K.; Rogers, S. E.; Turner, D.; Terry, A. E.; Treadgold, J.; King, S. M. Small Angle Neutron Scattering Using Sans2d. *Neutron News* **2011**, *22*, 19−21.
(33) http://www.mantidproject.org.
(34) Wignall, G. D.; Bates, F. S. Absolute calibration of small-angle neutron scattering data. *J. Appl. Crystallogr.* **1987**, *20*, 28−40.
(35) Benoit, H. The diffusion of light by polymers dissolved in a good solvent. *Comptes Rendus* **1957**, *245*, 2244−2247.
(36) Hammouda, B. SANS from homogeneous polymer mixtures: A unified overview. *Adv. Polym. Sci.* **1993**, *106*, 87−133.
(37) Flory, P. J. *Principles of Polymer Chemistry*; Cornell University Press: Ithaca, NY, 1953.
(38) Hammouda, B.; Ho, D.; Kline, S. SANS from Poly(ethylene oxide)/Water Systems. *Macromolecules* **2002**, *35*, 8578−8585.
(39) Hammouda, B.; Jia, D.; Cheng, H. Single-Chain Conformation for Interacting Poly(N-isopropylacrylamide) in Aqueous Solution. *Open Access J. Sci. Technol.* **2015**, *3*, 101152.
(40) Cheng, H.; Wu, C.; Winnik, M. A. Kinetics of Reversible Aggregation of Soft Polymeric Particles in Dilute Dispersion. *Macromolecules* **2004**, *37*, 5127−5129.
(41) Gennes, P. G. D.; Witten, T. A. *Scaling Concepts in Polymer Physics*; Cornell University Press: 1979; pp 245−264.
(42) Hammouda, B.; Briber, R. M.; Bauer, B. J. Small angle neutron scattering from deuterated polystyrene/poly(vinylmethyl ether)/protonated polystyrene ternary polymer blends. *Polymer* **1992**, *33*, 1785−1787.
(43) Akcasu, A. Z.; Tombakoglu, M. Dynamics of copolymer and homopolymer mixtures in bulk and in solution via the random phase approximation. *Macromolecules* **1990**, *23*, 607−612.
(44) Hiemenz, P. C.; Lodge, T. P. *Polymer Chemistry*, 2nd ed.; CRC Press: 2007; pp 247−288.
(45) Wolf, B. A.; Willms, M. M. Measured and calculated solubility of polymers in mixed solvents: Co-nonsolvency. *Makromol. Chem.* **1978**, *179*, 2265−2277.
(46) Dixit, S.; Crain, J.; Poon, W. C. K.; Finney, J. L.; Soper, A. K. Molecular segregation observed in a concentrated alcohol-water solution. *Nature* **2002**, *416*, 829−832.
(47) Yamaguchi, T.; Takamuku, T.; Soper, A. K. Neutron Diffraction Study on Microinhomogeneities in Ethanol−Water Mixtures. *J. Neutron Res.* **2005**, *13*, 129−133.
(48) Scherzinger, C.; Lindner, P.; Keerl, M.; Richtering, W. Cononsolvency of Poly(N,N-diethylacrylamide) (PDEAAM) and Poly(N-isopropylacrylamide) (PNIPAM) Based Microgels in Water/Methanol Mixtures: Copolymer vs Core−Shell Microgel. *Macromolecules* **2010**, *43*, 6829−6833.
(49) Pang, J.; Yang, H.; Ma, J.; Cheng, R. Solvation Behaviors of N-Isopropylacrylamide in Water/Methanol Mixtures Revealed by Molecular Dynamics Simulations. *J. Phys. Chem. B* **2010**, *114*, 8652−8658.

DOI: 10.1021/acs.macromol.6b00785
Macromolecules 2016, 49, 5152−5159